Babes Bolyai University, Cluj-Napoca
Faculty of Physics
Department of Biomedical Physics

PhD Thesis Summary

The analysis of cellular fluctuations

PhD Student: **Luiza Buimaga-Iarinca**

Scientific Supervisor: **CS I Dr. Vasile V. Morariu**

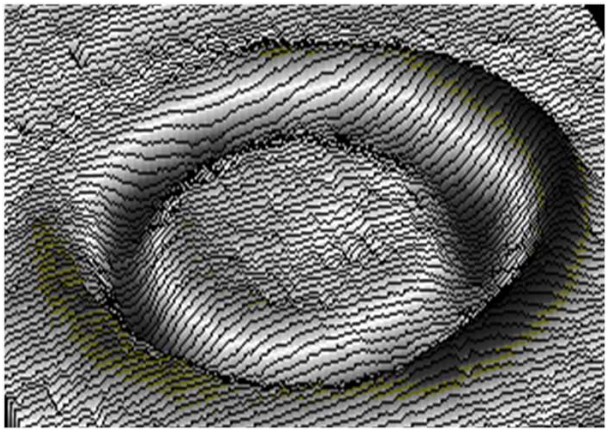

2010

Keywords

- Detrended fluctuation analysis, Temporal data series, Autoregressive modeling, Power spectrum, Trend, Interaction factor, Spectral correlation exponent;
- Erythrocyte, Cell membrane, Membranane fluctuations, Erythrocyte Flickering, Suspension medium.

Acknowledgements

I would like to address a special acknowledgement to Prof. Dr. Vasile V. Morariu in particular, for the caring and patience with which he oversaw the study, and for the scientific collaboration we had in the recent years.

Many thanks to Dr. Calin Vamos and his collaborators from the Institute of Computing Tiberiu Popoviciu, and also to Dr. Alexandru Pop, from the Astromomic Institute of the Romanian Academy for a fruitful collaboration in some research projects and surveys, part of this paper. Establishing the methodology for autoregressive model, the computer codes used in mathematical modeling, and also several scientific papers we published resulted in this collaboration.

For their benevolence, I would like to address my thanks to the management of the National Institute for Research and Development for Isotopic and Molecular Technologies from Cluj Napoca, where I worked on my doctoral thesis as the Institute supported the full tuition fees of my Doctoral School.

I would also like to thank my colleagues in the Department of Molecular and Biomolecular Physics for being there with relevant advice when I needed one.

Last, but not least, I must thank my family for the love and patience with which they surrounded me throughout the making of the study.

List of publications

ISI articles

1. Vasile V. Morariu, **Luiza Buimaga-Iarinca**, Calin Vamos, Stefan M. Soltuz, Detrended Fluctuation Analysis of autoregressive processes, Fluctuations and Noise Letters 7(3), L249-L255 (2007).

2. **Luiza Buimaga-Iarinca**, Vasile V. Morariu, Short range correlation of the erythrocyte membrane fluctuations, Journal of Physics: Conference Series 182 (2009) 012005 doi:10.1088/1742-6596/182/1/012005.

3. Vasile V. Morariu, Calin Vamos, Alexandru Pop, Stefan Soltuz, **Luiza Buimaga-Iarinca**, Autoregressive modeling of the variability of an active galaxy, Romanian Journal of Physics, 55 (7-8) 2010.

4. Vasile V. Morariu, **Luiza Buimaga-Iarinca**, Autoregressive modelilg of coding sequence lengths in bacterial genome, Fluctuation and Noise Letters, 9(1), L47-L59 (2010).

5. Vasile V. Morariu, Calin Vamos, Alexandru Pop, Stefan Soltuz, **Luiza Buimaga-Iarinca**, Oana Zainea, Autoregressive modeling of biological phenomena, Biophysical Review and Letters, 5(3), 109-128, 2010.

Other articles

1. V. V. Morariu, C. Craciun, Silvia Neamtu, **Luiza Iarinca**, and C. Mihali A fractal and long-range correlation analysis of plant nucleus ultrastructure, Rom. J. Biophys. 16(4), 243-252 (2006).

2. **Luiza Buimaga-Iarinca**, Autoregressive analysis of the erythrocyte flickering, Rom. J. Biophys 18(1), 67-72 (2008).

3. **Luiza Buimaga-Iarinca**, V.V. Morariu, Phosphate Buffered Saline-induced changes in red blood cells membrane fluctuations, Studia UBB, Physica, LIII(2)(2008).

4. **Luiza Buimaga-Iarinca**, Silvia Neamtu, Mihaela Mic, Ioan Turcu, Comparative analysis of Bacillus subtilis and Escherichia coli sakai genomes. The high order autoregressive method, Rom. J. Biophys., 20(3), 203-211 (2010).

Contents

1 Introduction

This study was designed on two levels, a mathematical and a biophysical one. From the mathematical point of view we have proposed a simple and robust autoregressive model which returns values similar to those returned by a complex mathematical model. One of the parameters (φ) proved to be the main quantitative indicator of correlations existing in the data series, so it can be exploited to investigate various processes of the fluctuating processes. The model was validated by applying it to some data in the specialized literature. Next we it use to investigate the correlation existing in the genome at the coding secquences level. By simultaneously applying the mathematical methods and models in question, we highlighted differences in the fluctuation of erythrocyte membranes suspended in different media.

The first part provides an overview of the mathematical methods and models. It requires a prior understanding of some mathematical methods used to investigate the correlation of time series consisting of the consecutive values for large diameters of red cells. The second part of the work focuses on validating the mathematical models by analysing of specific real cases. In the third part is presented a detailed analysis on the way the membrane of red blood cells fluctuates.

Part I

Methods and mathematical models used to investigate fluctuations

2 Power spectrum analysis - Fast Fourier Transform

The power spectrum calculation is done by FFT (Fast Fourier Transform). FFT is an efficient method used to compute Discrete Fourier Transform (DFT) and its inverse. Here sequential data sets are investigated by a decomposition accordind to the frequency. Spectral correlation exponent is a parameter characteristic to stationary series. A time series can be considered stationary if mean, standard deviation and correlation function are time invariant. Data series pertaining to real phenomena, however, shows noises and trends. This can bring

additional correlations into the system. Therefore it is necessary to undertake further analysis to eliminate them.

3 Detrended Fluctuation Analysis

3.1 What is DFA?

Detrended Fluctuation Analysis is the method of analysis generally used to investigate the time series characteristic to real phenomena, which contain noise and trends [7]. The main parameter used in DFA is the *scaling exponent* (α) which describes the correlation properties of data series.

DFA advantage over other methods of calculation is that it allows detection of long range correlation of noisy data series. Also DFA avoid false detection of apparent long-range correlations which are an artifact of non-stationarity. DFA allows identification of different states of the same system depending on its scaling behavior [8].

Note that the DFA algorithm works better with certain types of non-stationarities, especially for series with trends without sudden changes. However, there are cases where this method canot fully extract the trends [9].

3.2 The relationship between spectral correlation exponent and scaling coefficient

Between α (the scaling exponent) calculated by DFA and β (spectral correlation exponent) calculated by FFT there is the following relation: $\beta = 2\alpha - 1$ [12] . This relationship is valid only for stationary series.

3.3 Effects of noise and trends on DFA

The influence of trends [17] shows that the only where DFA is ineffective is the one in which sudden jumps occur in series (pronounced peaks).

DFA method can be used on nonstationary series only as a simple tool to investigate the type of correlation which exists in series. Complex information about the laws that govern the phenomenon under investigation may be obtained by applying only elaborated analytical methods.

4 Autoregressive models

4.1 AR1 Process

An first order autoregressive process is defined by:

$$X_t = c + \varphi x_{t-1} + \upsilon_t \tag{1}$$

where υ_t is a white noise process with zero mean and σ^2, x_{t-1} is a term in series and c is a constant [19]. The process is called stationary if $|\varphi| < 1$. If $|\varphi| = 1$ then X_t shows a unit root and can be considered random process.

4.2 AR_p Process

In this case the characteristic equation takes the form:

$$X_t = \sum_{i-1}^{p} \varphi_i X_{t-i} + \upsilon_t. \tag{2}$$

The base is the parameter φ_i where $i = 1, ..., p$. The process is stationary if the condition $|\varphi| < 1$ is fulfilled.

4.3 Spectral feature of the AR model. Infinite length and finite length

A discrete stochastic process, having $X_n, n = 0, 1, 2...$ is called autoregressive process of order p [22], denoted *AR(p)*, if X_n is stationary for any n:

$$X_n - \varphi_1 X_{n-1} - ... - \varphi_p X_{n-p} = Z_n \tag{3}$$

where Z_n is a Gaussian white noise with zero mean and variance σ^2.

The real parameters φ_i, *i = 1 ,..., p*, can be interpreted as a measure of the influence of the stochastic process term on his neighbor of order *i*. The *ARp* properties have been studied in detail [22].

Equation 3 has a singular solution if the polynomial $\Phi(z) = 1 - \varphi_1 z - ... - \varphi_p z^p$ has no roots z with $|z| = 1$ [23]. If $\Phi(z) \neq 1$ for all $|z| < 1$ the process is causal, *i.e.* x_n random variables can be expressed only as a function of noise values in the previous stages. The study is detailed by Vamos and colleagues [27].

The spectral density of an *ARp* process is:

$$f(\upsilon) = \frac{\sigma^2}{2\pi} \frac{1}{|\Phi(e^{-2\pi i\upsilon})|^2}, -0.5 < \upsilon < 0.5 \tag{4}$$

where υ is the characteristic frequency. For an $AR1$ process, spectral density in equation 4 becomes:

$$f(\upsilon) = \frac{\sigma^2}{2\pi} \frac{1}{1 + \varphi^2 - 2\varphi cos 2\pi\upsilon}, -0.5 < \upsilon < 0.5 \tag{5}$$

where φ in this case is the unique interaction factor. The formula mentioned above is correct only for finite-length real stochastic processes.

Time series that exist in practice have a finite length and can be considered segments from a stochastic process of infinite length. Thus, we can replace the terms of the equations 4 and 5 such that becomes possible to analyze a sample of finite length $X_n, n = 1, 2, ..., N$ extracted from a series of infinite length $X_n, n = 0, \pm 1, \pm 2, ...$

A detailed analysis of the power spectrum of the $AR1$ process and the influence of finite length is given in [24], [25], [26].

We present below some issues relevant to further understanding of the analysis detailed in this study.

By definition, the spectral density estimator is the periodogram:

$$I_N(\upsilon) = |A_N(\upsilon)|^2 \tag{6}$$

where $A_N(\upsilon)$ is the discrete Fourier transform of the series:

$$A_N(\upsilon) = \frac{1}{\sqrt{N}} \sum_{n-1}^{N} X_n e^{2\pi i n \upsilon} \tag{7}$$

Since the series is finite we have only N independent values $A_N(\upsilon)$ and $I_N(\upsilon)$. Generally, these values are calculated for Fourier frequencies $\upsilon_j = j/N$, where j is an integer that satisfies the condition $-0.5 < \upsilon_j < 0.5$. The periodogram of an $AR(p)$ process is an estimator of spectral density:

$$\lim_{N\to\infty} \langle I_N(\upsilon_j) \rangle = 2\pi f(\upsilon) \tag{8}$$

where $(\upsilon_j - 0.5N) < \upsilon \leq (\upsilon_j + 0.5N)$.

While the series length N increases (as long distance is kept constant) averaged periodogram becomes a better approximation of spectral density. We note that a single periodogram is not a consistent estimator because it does not converges in probability with the spectral density. Here standard deviation $I_N(\upsilon_j)$ does not tend to zero and two distinct

values of the periodogram are not correlated, no matter how closeness are the calculated values for frequency. Typically spectral density and periodogram are represented in double logarithmic coordinates. Logarithmic coordinates strongly distort the shape of the graph and near the origin it is transformed into an infinite range, the value of $f(0)$ not being represented graphically.

For a total number of n terms, the first value of the spectral density is obtained at the lowest frequency $\upsilon_{min} = 1/N$. Figure 1 shows the spectral density for $N = 1024$ and $\sigma = 1$, at different values of φ. For $\varphi \geq 0.90$ most of the power spectrum is almost linear having a slope equal to -2, which corresponds to $\beta = 2$.

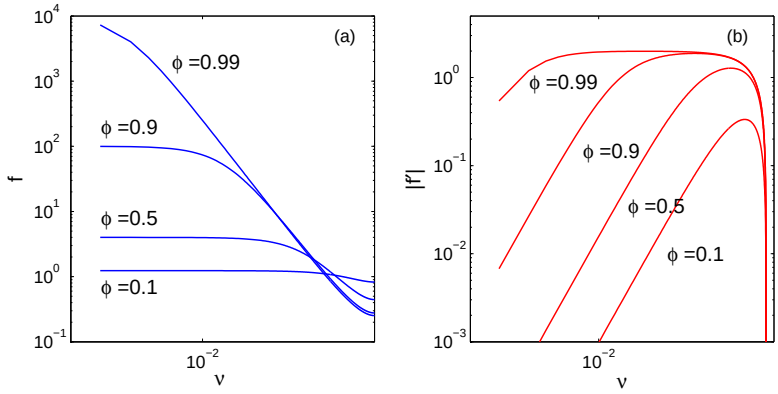

Figure 1: Spectral density and its absolute derivative value for $AR1$ process with $N = 1024$, $\sigma = 1$ and different values of the interaction factor φ.

The figure 1 shows the spectral density derived in double-logarithmic coordinates.This usefull to verify the behavior of $AR1$ spectrum, :

$$f^{|}(\upsilon) = -\upsilon \frac{d}{d\upsilon} ln(f(\upsilon)) \tag{9}$$

It may be noted that for $\varphi = 0.9$ there is a region where $f^{|} \cong 2$ (see figure 1,left). Here is only one maximum value of $f^{|}$ for $\varphi < 0.9$ which corresponds to the central (fractal) part of the power spectrum. For low frequencies, spectral density of an $AR1$ process is highly flattened in double-logarithmic coordinates so that appears a plateau (see Figure 1) with the value given by:

$$f(0) = \frac{\sigma^2}{2\pi(1-\varphi)^2} \tag{10}$$

From equation 7 it follows that the small values of υ correspond to the plateau regions where the variable term in the denominator may be neglected in comparison with

the constant term. Using the quadratic approximation of cosine function, the need for graphical representation of the power spectrum $AR1$ is to have a plateau $\upsilon < (1-\varphi)/2\pi\sqrt{\varphi}$. If φ goes to 1, the plateau occurs at lower values of frequency. On the other hand, if N is large enough, the periodogram has the plateau at lower values of frequency.

We consider a time series $x_n, n = 1, 2, ..., N$ obtained from an $AR1$ autoregressive process. If we apply discrete Fourier transform to the x_n series and compute the periodogram, then we get the values randomly distributed around the spectral density of the $AR1$ process.

The periodograms are not consistent estimators, so the fluctuations around the theoretical spectral density values are not reduced by increasing the length N of the series.

Consistent estimation of the spectral density may be obtained using averaged periodograms on intervals with order of magnitude about $\sqrt{N}$. Choosing the optimum weight function is a difficult task. If the periodogram is smoothed too much, then the bias with respect the theoretical spectrum can become large. From various weight functions the simplest one is used, *i.e.* averaging with equal weights on symmetric intervals containing M Fourier frequencies, with $M = 1, 3, 5, ..., 21$. The averaged periodogram contains *N-M+1* values, because for the first and last $(M-1)/2$ values of the periodogram the symmetric averaging cannot be performed.

4.4 Effects of noise and trends on AR

We did a study in which we generated artificial series having $\varphi \in [0.3..0.9]$ and data dispersion σ equal to 0.5. These series were generated with our software developed in MATLAB R2008a [28]. We added white noise generated in OriginPro8, with intensities ranging between 10^{-2} and 10^2. In addition, we added two trends, one polynomial $p = 2x^2 + 3x + 4$ and one sinus on the initial series and on series already containing noise over.

Noise and trends may hide the data from series belonging to natural phenomena. Then the autoregressive algorithm will return incorrect values. As a result, the first thing we recommend when there are analyzed data pertaining to real phenomena is to remove the trend. The resulted series, free of noise and trends, are those that may be subject of autoregressive analysis.

5 The relationship between AR and DFA

5.1 The relationship between $AR1$ and DFA

How can we identify the type of correlation in a series, and which is the connection between these models?

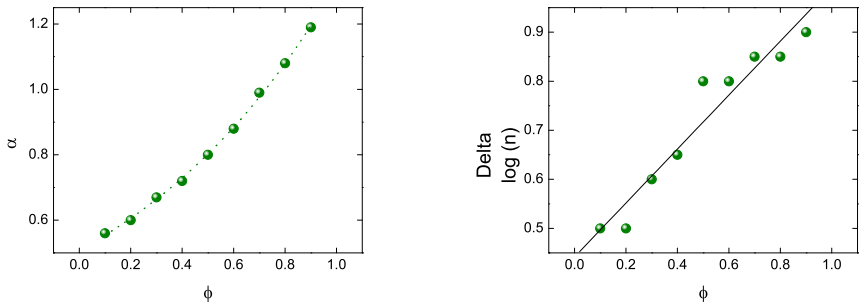

Figure 2: (a) Dependence of the interaction factor by the scaling exponent of the first correlation segment is exponential. (b) Dependence of the interaction factor by the first correlation segment length is almost linear.

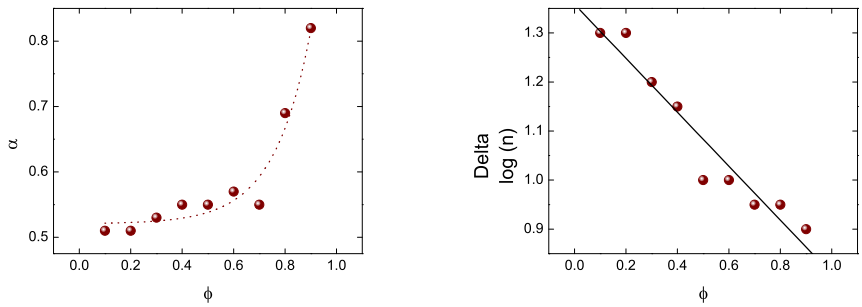

Figure 3: (a) Dependence of the interaction factor by the scaling exponent of the second segment is also exponential correlation; (b) Dependence of interaction factor by the length of the second correlation segment is also almost linear, having the slope of the linear inverse to the first segment slope value.

In our analysis were generated 1000 terms series having a known interaction factor [11]. For all that series, the dispersion had the value $\sigma = 1$. These series may look different although they have the same characteristics of interaction between terms. Detrended

fluctuations analysis of these series shows different forms in double-logarithmic coordinates representation. That's why we worked with their arithmetic average.

Each of the DFA representations in double-logarithmic coordinates is nonlinear. Note also that the slope (the correlation exponent) increases with φ.

The DFA representation shows two correlation segments for every $\varphi \in [1..9]$. The first segment corresponds to the correlation between closer terms and the second belongs to the correlation between distance terms. The lengths of these segments also varies for each case (see Figure 2).

5.2 The relationship between ARp and DFA

If the generation of series is based on an ARp algorithm, the analysis becomes more complicated. In this case, due to the scattering that occurs in the DFA representation in double-logarithmic coordinates, we had to generate ten series for each model. We used their arithmetic average.

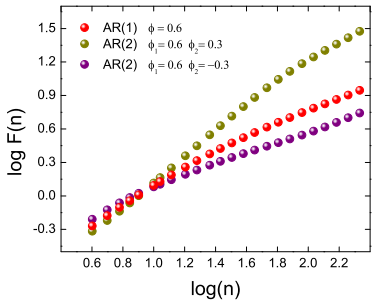

Figure 4: Comparision betbeen $AR1$ ($\varphi = 0.6$), $AR2$ ($\varphi_1 = 0.6$ and $\varphi_2 = 0.3$), respectively $AR2$ ($\varphi_1 = 0.6$ and $\varphi_2 = -0.3$).

In figure 4 we showed how the DFA representation varies from $AR2$ with $\varphi_1 = 0.6$ and $\varphi_2 = 0.3$, to $AR1$ with $\varphi = 0.6$. Note that both α_1 and α_2 differs strongly with each other (we refer to the scaling exponents belonging to the same $AR2$ with two different parameters φ_2). The degree of long distance correlation is also different for this set of parameters (see Figure 5).

Higher order autoregressive models have a complex correlation. Therefore they cannot be described in a simple way.

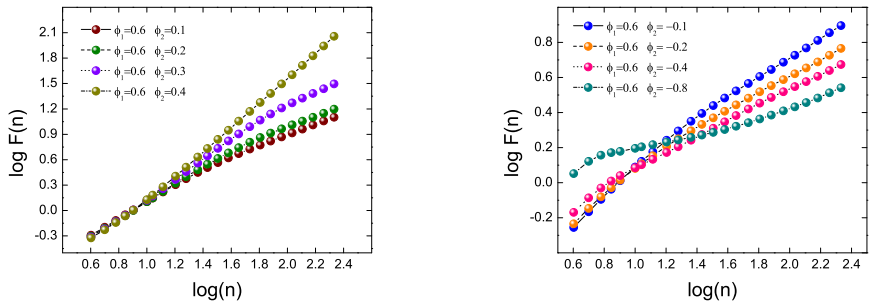

Figure 5: (a) DFA for $AR2$ with $\varphi_1 = 0.6$ and $\varphi_2 > 0$. (b) DFA for $AR2$ with $\varphi_1 = 0.6$ and $\varphi_2 < 0$. For $\varphi_2 > 0$ one can observe a linear dependence of the slope value for long distance correlation (α_2) by the growth of the interaction factor values. For $\varphi_2 < 0$ the law is much more complex.

Part II

Validation of AR models and calculation procedures for series belonging to real phenomena

6 Analysis of the X-ray light curves data series of the active galaxy NGC5506

We used several real phenomena in order to test the methodology described above. These include the X-ray light curves data series of the active galaxy NGC5506 and the analysis of the bacterial genome.

Complex autoregressive analysis was made for X-ray light curves of the active galaxy NGC5506 by Koning and coleagues [39]. We compared the results obtained by their analysis method with the method proposed by us to validate our method. We used the same data as in [39]. Data were extracted from archive *EM Hearc Exosat* for Seyfert galaxy NGC5506.

6.1 Data series

The sequence of operations used to process the data can be summarized as follows:

1. The data series was detrended by extracting different polynomial fitting;
2. The FFT transform of the series was performed;
3. The resulting periodogram was mediated to 1 up to 21 terms;
4. The spectrum was fitted by using the $AR1$ model. The final parameters are the interaction factor φ and dispersion σ. Their values depend on the polynomial degree used in the detrending procedure.
5. We choosed the optimum values of φ and σ depending on the number of averaged terms and on the detrending polynomial degree.

6.2 The $AR1$ fitting procedure of the X-ray emission of NGC5506 galaxy

In our analysis, we start by removing the deterministic trend from the signal. We note that it has not been extracted by Timmer and Konig in their analysis.

Three different trends can be obtained from three different polynomial fitting (see Figure 6).

These polynomials degree is the minimum degree of a class of polynomial trends, q, which have very similar shapes. We note that the trend does not change its shape with the monotonically increasing of the polynomial trend. At a fixed degree of the polynomial trend changes significantly, while at higer degree the trend remains practically unchanged. The trend is reduced to a constant equal to the average of the time series when $q = 0$.

Averaging procedures lead to loss data at low frequencies (they form a plateau in autoregressive modeling). At higher frequencies than the cutoff frequency ($\nu_0 = 0.02$) the periodograms turns to white noise spectrum. Only in the region of the spectrum with $\nu > \nu_0$ the process can be modeled with an $AR1$. The values of $\varphi = 0.991$, $\sigma = 0.757$ and $\varphi = 0.985$, $\sigma = 0.744$ are obtained from fit in the region of low frequencies. There are very closer to those reported by Konig and Timmer.

The average range of periodogram also has a strong influence on the $AR1$ model parameters. This dependence is presented as a function of M for various degrees of the

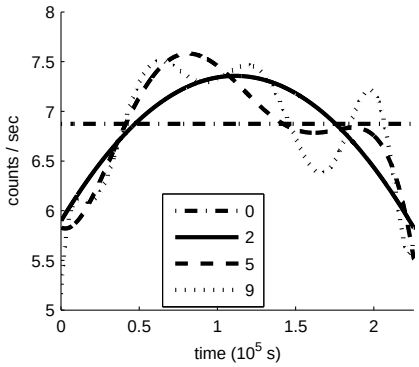

Figure 6: Time series of X-ray emission of the active galaxy NGC5506. The trends is obtained by four different polynomial fitting (0, 2, 5 and 9 degree). The trend is reduced to a constant when the polynomial degree $q = 0$. For $q = 2$, the polynomial trend describes the overall shape of the signal. For $q = 5$, the polynomial describe the different behavior for the first and the second part of the signal. Polynomial trend can follow the signal details when $q = 9$.

polynomial trend. For small values of M, the values of φ and σ are quite different. Their variability is significantly reduced for $M > 9$, when the average procedure of the periodogram eliminate some fluctuations. This is why in this study, we used $M = 11$.

Another analyzed parameter is the cutting frequency ν_0. We note that at frequencies below 0.02, the periodogram shows oscillations that may be caused by white noise with higher frequencies. For comparison with Koning results, we will use $q = 0$ because Koning and Timmer have not removed the deterministic trends from the signal. The relative error is 0.2% for φ and 5% for σ and confirms the validity of autoregressive spectral modeling proposed by us.

6.3 Discussion

We used the model described in the previous chapter to characterize the X-ray emission of a galaxy. Our calculation procedure, simpler, lead to similar results to those obtained by more elaborate calculations. Parameter φ has proved to be very sensitive, so it can be exploited to investigate different effects of fluctuating systems.

7 Autoregressive analysis of bacterial genomes

Bacterial chromosome have a relatively simple structure and consists of a set of coding sequences (CDS) and noncoding sequences (NCDS). Each sequence consists of a series of specific bases. Coding sequences represents genes and dominates the total content of bases in the bacterial chromosome. Detrended fluctuation analysis of the CDS length shows that the bacterial genome has a short range correlation [47].

7.1 Bacterial genome

We analyzed these types of series:

1. Entire series, consisting of a natural sequence of the genome coding sequences, $l(+/-)$;
2. Series of the CDS lenghts on the *plus* strand, $l(+)$, respectively
3. Series of the CDS lenghts on the *minus* strand, $l(-)$.

These data were extracted from the *European Molecular Biology Laboratory (EMBL)* site.

7.2 Strategy of analysis

The sequence of operations can be summarized as follows:

1. The series was detrended by extracting different polynomial trends;
2. It was applyed the Discrete Fourier Transform;
3. The periodogram was averaged between $M = 1$ and 21 terms;
4. The spectrum was fited by using an $AR1$ model. If the data can be described with the model, we choosed the final values for φ and σ.
5. This procedure was applied to $l(+/-)$, $l(+)$ and $l(-)$.

7.3 Autoregressive analysis of the coding sequence lengths of the bacterial genome

Let us summarize our conclusions on the bacterial genome analysis. The autoregressive model parameter values can vary between $0 < \varphi < 1$. In the case of bacteria and archaea these varions are between 0.52 for *Bacillus subtilis* and almost zero for some lines of *Haemophilus influenzae* and *Helicobacter pylori* (our work). This means that the strength of interaction between the terms given by CDS length series varies in a wide spectrum, from almost zero interaction to strong interaction. Moreover, this interaction is sensitive to strand *plus* or *minus* and to the differences between species.

7.4 Biological significance of the autoregressive model

We propose as possible explanation of the validity of the autoregressive model in the bacterial genome analysis the structural organization of the genome in *operons*[1]. Genes are organized in operons with the same functionality [98]. Since operons have comparable lengths, we expect CDS lengths to present local correlations.

Part III

Red blood cell membrane fluctuations

8 Biophysics and biochemistry of the erythrocyte membrane dynamics

Cells have specialized functions that depend on the role they fulfill in the body [55]. All the cells, either prokaryotic or eukaryotic, have a membrane that wraps them, separating from the external environment and medium, and mediates the inputs and outputs of matter and energy.

Cell membrane is a bilipidic layer having a selective permeability. It contain a wide variety of biological molecules, especially proteins and lipids that are involved in many biological processes such as cell adhesion, ion channel conductivity or cellular signal issue.

[1]There are functioning units of genomic material containing a cluster of genes under the control of a single regulatory signal.

The most general representation of erythrocyte membrane structure is the *fluid mosaic model*[2] [59].

8.1 Human erythrocyte

A typical human erythrocyte has a diameter of 6-8 μm and a thickness of about 2μm, and is much thinner than most other human cells. These cells have a volume of around 90 fL and an area of approximately 136 μm^2. They can turn into a sphere with a volume of 150 fL without membrane extension.

A red blood cell takes about 20 seconds per traffic cycle [63], [64], [66]. These cells are otherwise anucleated so the protein biosynthesis does not occur for eritocite. There is however a recent study which indicates the existence of the biochemical apparatus necessary for the biosynthesis of the protein [65].

Human red blood cells are produced by a process called *erythropoiesis* and become mature cells in seven days from stem cells. The RBCs remain in the blood cycle for a period of about 100-120 days. At the end of their life, they turns to sferocite and are removed from circulation by the spleen, which acts as a mechanical filter.

8.2 Red blood cells flickering

Spontaneous fluctuations in the erythrocytes surfaces were observed since the end of last century [70] by optical microscope examination. The phenomenon is due to undulations of the cell surface (membrane undulations) and is called *erythrocytes flickering*, occuring with a frequency between 0.3 and 30 Hz.

Assumptions about the mode of fluctuation are very different. Based on the data analysis of the autocerelation function, Zeman [71] concludes that erythrocyte requires ATP to ensure a free deformation regime. Tuvia [72] (1992) shows that producing MgATP is directly related to cell fluctuation amplitude. In addition, he shows that oxygenation - de-oxygenation cell cycle plays an important role in modulating membrane fluctuations, de-oxygenation involving reduction of the fluctuation amplitude [73].

The methodology of investigation was later developed by monitoring the cell edge fluctuations [74] by *flickering spectroscopy*. This method allows a very precise determination of elastic properties of the cell membrane. It has been shown that environmental variation

[2]It was proposed by S.J. Singer and Garth Nicolson and assumes that biological membranes can be considered a two-dimensional fluid in which all lipids and proteins can move more or less freely.

of viscosity induces changes in the fluctuation characteristics. As the growing concentration of macromolecules (dextran 70, dextran 500, dextran 2000, cellulose) from solution, the amplitude of fluctuations decreases. Data acquisition method used is Point Dark Field Microscopy, and involves the recording of the quantity of light that passes through the membrane. Note that in this case the cell is fixed on the substrate, which means that the membrane does not fluctuate freely.

Fluctuations of the cell membrane depend on the suspension viscosity [75]. On the other hand, a fundamental role in stimulating fluctuations is related to *F actin*, a component of the cytoskeleton [76]. As a result, the membrane fluctuations are implicitly linked to the suspension viscosity and the cytoskeleton fluctuations.

Regarding the spectral domain, it is considered that the phenomenon of flickering occurs within 0.3 to 30 Hz [77]. Gaczinska *et al* signals the existence of some very slow oscillations with periods longer than 1.5 hours [78]. These areas of frequently, called long ultradiene rhythms, have been identified up to a range of 13 to 18 hours [79]. Unlike previous studies, data analysis in question failed to emphasize the oscillations themselves, but only noise type 1/f.

The accelerated development of the microscopy in recent years has led to more complex investigation of cellular fluctuations. There have been revealed fluctuations and other phenomena that influence the membrane, such as reorganization of the cytoskeleton in red blood cells and hemoglobin distribution un-uniformity by interference imaging

It was found that low frequency variations of erythrocyte membrane (0.1-0.6 Hz) is due to membrane - plasma interactions, while higher frequency fluctuations (20-26 Hz) are correlated with membrane vesicles trips [80]. Therefore different optical techniques were put in place for investigating fluctuations in membrane: FPM (Fourier Phase Microscopy) [81], HPM (Hilbert Phase Microscopy) [82], DPM (Difraction Phase Microscopy) [83] and FFTM (Fast Fourier Phase Microscopy) [84]. A significant advance in modeling the flickering phenomenon and mechanical properties, correlated with the statistical properties of the cell membrane fluctuations, was made by developement of the AFM (Atomic Force Microscopy), which led to the possibility to investigate the fluctuations of the cells that are no longer attached to the substrate. Through these studies was emphasized independent existence of dynamic subdomains in the cell, which fluctuates in different frequency regimes [85]. These highly accurate optical interferometry techniques (nano scale and milliseconds) have also led to the identification of correlations between membrane properties at spatial and temporal cell membrane viscoelastic properties [85].

9 Investigation of the cell membrane fluctuations

We followed the red blood cell membrane fluctuations by analyzing the two parameters: spectral correlation exponent (α) [95] and the interaction factor (φ) [94]. was calculated by Detrended Fluctuation Analysis while φ was obtained by spectral analysis and modeling with the autoregressive model. Another characterization of membrane fluctuations in different environments was done by analyzing the amplitude of fluctuation.

Analysis of cell membrane fluctuations was made for different classes of red cells, as follows:

- Healthy cells suspended in their natural environment (blood plasma) and in an artificial environment, (PBS - Phosphate buffered saline)[3];
- Healthy cells suspended in the two environments as above, in which drugs were added (chemical factors);
- Aging cells *in vitro*.

9.1 Experimental setup

The experimental setup consists of the following main components:

- Research microscope;
- Counting cell;
- CCD Camera;
- Computer.

The used microscope is an inverted microscope, Optika XDS-2 type, and the CCD camera is OptikamPRO3.

9.2 The procedure to define the edges of erythrocytes

The program used to delimit the edges of cell by the suspension environment is Image J [89],[90], with the plugins Shape descriptor [91]. It is based on the algorithm proposed by Russ [92]. Surface particle calculation is done by effectively counting pixels in the image.

[3]PBS is used routinely in the laboratory for investigation of various properties of cells. Through this study we demonstrated that, in terms of membrane fluctuation characteristics, PBS is not an optimal environment.

9.3 Biological sample preparation

9.3.1 Suspension media

Red blood cell membrane fluctuations were followed on erythrocyte suspensions, prepared from human blood, collected on anticoagulant (sodium citrate 3.8 %) from healthy donors. Whole blood was centrifuged 8 min at 3000 rpm and cells were separated from plasma. White blood cells and platelets were removed. Erythrocyte sediment was ultra centrifuged 3 min at 4500 rpm to obtain a concentrate of red blood cells of about 99.9 %. Plasma was also ultra centrifuged 5 min at 7000 rpm to get a pure plasma. From this erythrocyte sediment, there were prepared cell suspension by resuspension of erythrocytes in plasma at dilutions high enough to avoid cell aggregation. Alternatively the suspension medium was a phosphate buffer solution (PBS) containing 20 ml of phosphate buffer to 100 mM NaCl (0.76 g), BSA (100mg) and glucose (0.18 g) per 100 ml solution[4].

9.3.2 Chemicals used in the investigations

Epinephrine or adrenaline 1mg/ml in solution. It is a hormone that plays a central role in short - term stress reactions in the body. His reactions are mediated by adrenergic receptors located on several cell - type surfaces. The action of this hormone is limited and reversible, disappearing completely in about one hour after administration.

Lidocaine or xiline, in solution, 100mg/10ml. It is a local anesthetic amino - amide type, lasting effect of about 1.5 - 2 hours for most patients. It works by blocking fast sodium channels ($Na+$) in cell membranes.

9.3.3 Types of experiments

We imagined 5 scenaries in order to detect the behaviour of the red cells in physiological conditions as follows:

1. **Healthy cells re-suspended in plasma**: human blood is collected on anticoagulant (sodium citrate 3.8) derived from healthy donors. It was centrifuged for 8 min at 3000 rpm to separate plasma. White cells and platelets ware removed. The sediment was ultra-centrifuged 3 min at 4500 rpm. Plasma was also ultra centrifuged 5 min at 7000

[4] 1 liter of Phosphate-buffered saline (PBS buffer) could be prepared from 8 g NaCl, 0.2 g KCl, 1.44 g Na_2HPO_4 and 0.24 g of KH_2PO_4 dissolved in 800 ml distilled H_2O. We adjusted the pH to 7.4 with HCl and added H_2O to a liter.

rpm. Erythrocyte cell suspensions were prepared by resuspension of erythrocytes in plasma at dilutions sufficient to avoid cell aggregation.

2. **Healthy cells suspended in PBS**: red blood cells from healthy donors were separated from plasma by centrifugation, 5 min at 4000 rpm and then washed three times with phosphate buffer solution which was removed by centrifugation 5 min at 4000 rpm. Last centrifugation lasted 10 min. A small number of red blood cells were re-suspended in PBS.

3. **Cells re-suspended in plasma with chemicals**: whole blood was centrifuged for 5 min at 4000 rpm to separate plasma from red blood cells sediment. White cells and platelets were removed. Plasma was ultra-centifuged 5 min at 7000 rpm. It was calculated the dose of medication to get maximum effect for epinephrine and lidocaine (0.5 μl epinephrine 250 μl plasma and 5 μl lidocaine 250 μl plasma). The erythrocytes suspended in those media were incubated 20 min at a temperature of 37 degrees C.

4. **Cells re-suspended in PBS with chemicals**: red blood cells from healthy donors were separated from plasma by centrifugation, 5 min at 4000 rpm and then washed three times with phosphate buffer solution. Washed erythrocytes were re-suspended in PBS with epinephrine (0.5 μl epinephrine to 250 μl PBS) and PBS with lidocaine (5 μl lidocaine to 250 μl PBS). The suspension was incubated 20 min at a temperature of 37 degrees C.

5. **Blood aged** *in vitro*: blood was collected on anticoagulant (sodium citrate) from healthy individuals. To highlight the effects of aging, experiments were conducted in several stages:

   (a) Immediately after sampling: erythrocytes were separated from plasma by centrifugation (5 min at 4000 rpm), plasma was ultra centrifuged (5 min at 7000 rpm, erythrocytes were re-suspended in plasma, at a high dilution to avoid the phenomenon of aggregation.

   (b) Blood 6:00 aging: blood processing was performed at 6 hours after harvest, during which time blood sample was stored at room temperature (about 21 degrees C), sample processing module is identical to that for fresh blood.

   (c) 24:00 Aging Blood: Blood processing was done at 24 hours after harvest, during which time blood sample was stored at room temperature (about 21 degrees C),

sample processing module is identical to the previous samples.

(d) 48:00 Aging Blood: Blood processing was done at 48 hours after harvest, during which time blood sample was stored at room temperature (about 21 degrees C).

9.4 Recording images

To analyze the dynamics of erythrocyte membrane we performed the following steps:

1. We recorded sets of 1000 sequential images for each erythrocyte. Sampling rate was 5 fps. Resolution was 2048 x 1536 pixels for maximum image that captured a total of 10 RBCs. This series of images was transformed into stacks of 1000 images using ImageJ.

2. Stacks were processed for analysis using treshold command that turns the color image in black and white and highlight the cell area.

3. With the Analyze Particle command we defined the cell area of the background image (for all 1000 images).

4. These simple geometric shape was analyzed with both Analyze Particle plugins, and Shape Descriptor10 plugins[5].

9.5 Mathematical modeling

The data series consist of large diameter value of each cell. These values were acquired for approximately 60 cell suspended in each medium. Data analysis was done as follows:

1. FFT transform was applied to data sets and the spectral exponent of correlation was calculated.

2. DFA analysis was carried out and calculated the scaling exponent.

3. The power spectrum obtained with the discrete FFT transform was modeled by autoregressive models of order 1 and higher orders.

[5]These plugins do not fart plugins-standard package Image J, but can be found on the official website of the program.

10 Results and discussion

10.1 Healthy cells suspended in plasma and PBS

After detrending, the data were transferred to Origin and plotted.

For cells suspended in plasma, a very strong correlation is observed in the first segment with $\alpha_1 = 0.96 \pm 0.01$ for the area, $\alpha_1 = 0.98 \pm 0.02$ for large D and $\alpha_1 = 0.85 \pm 0.01$ for small D (see Figure 7).

For distant terms, the correlation remains strong, but ceases to be of type 1/f. $\alpha_2 = 1.32 \pm 0.02$ for the area, $\alpha_2 = 1.14 \pm 0.01$ for large D and $\alpha_1 = 1.21 \pm 0.01$ for small d (see Figure 8).

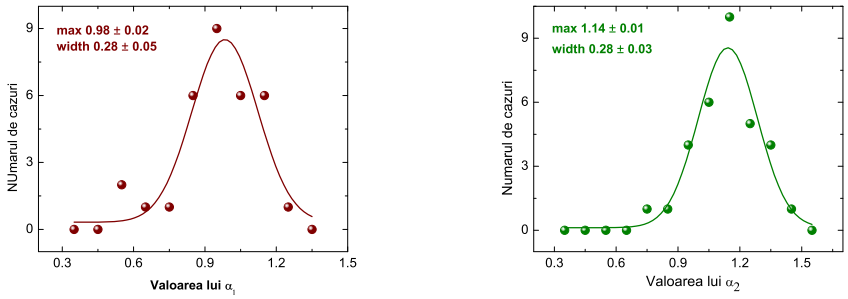

Figure 7: Gaussian distribution of the correlation between the closer and distant terms. Red blood cells are suspended in plasma.

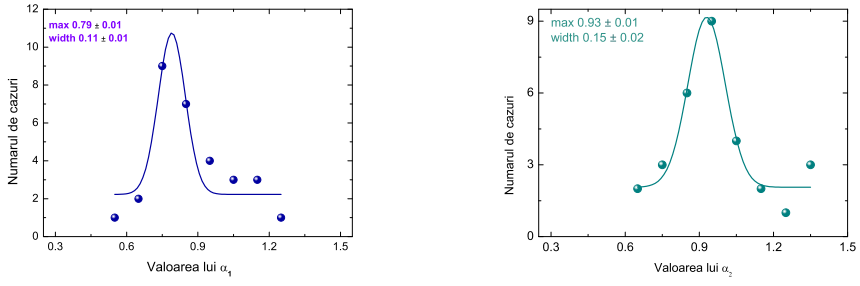

Figure 8: Gaussian distribution of the correlation between the closer and distant terms. Red blood cells are suspended in PBS.

We calculated the Gaussian distributions for lots of 60 cells immersed in plasma and PBS. It reveals a statistically significant difference between correlations, the *Two Independent*

Sample t-Test parameter being $P = 0.00896$. Median values for $\alpha_{1plasma} = 1.00 \pm 0.00$ and for $\alpha_{1PBS} = 0.96 \pm 0.01$. The results are shown in Figure 10.

Differences between correlation exponent values for the two environments indicate that the mode of membrane fluctuation is strongly affected by the introduction of the cell in an artificial environment. The degree of heterogeneity of the cell population decreases rapidly, Gaussian width being 0.28 ± 0.02 for plasma and decreasing to 0.12 ± 0.02 in the case of PBS.

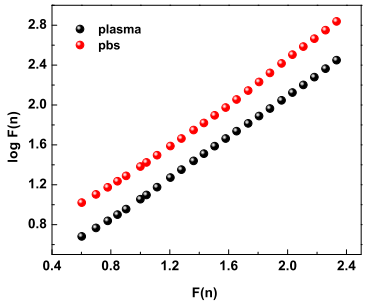

Figure 9: Averaged DFA for all cells suspended in plasma (black) and PBS (red). PBS amplitude fluctuations, described by the function *log F(n)* is greater because of lower density of PBS than plasma.

When DFA is represented as the average values for the entire group of 50 cells (for cells suspended in plasma and for those suspended in PBS) we observed that the amplitude of the fluctuations varies from plasma to PBS (see Figure 9). In PBS, the cell fluctuates larger considering the average density of matter. In plasma, the liquid density is greater than PBS so it limits the width of membrane fluctuations.

In order to perform autoregressive modeling we applied the discrete Fourier transform on series from which we extracted in advance the trend. It was approximated by a polynomial of degree 10. Power spectrum was averaged over 21 terms to emphasize the shape. The first remark is that can be done in averaging is that the spectrum shows deviations from *1/f* type power law. For the cells suspended in plasma, or for those suspended in PBS the spectrum cannot be fitted linear. Best fitting model is the autoregressive of order one.

Gaussian shaping of the interaction factors resulted from AR1 (Figure 10) confirm the results obtained with DFA. Median for φ_{plasma} is 0.78 ± 0.00 and for φ_{PBS} is 0.73 ± 0.01. P parameter value is statistically significant $P = 0.056$.

The suspension of red blood cells in artificial environment influences the membrane

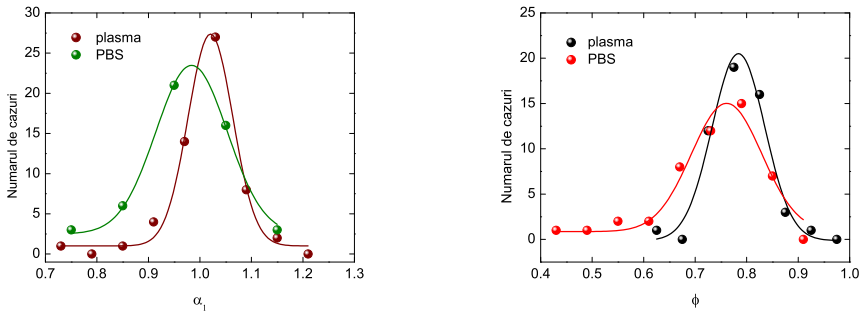

Figure 10: (a) Compared values of the Gaussian distribution for the correlation exponent between cells suspended in plasma (black) and PBS (red), (b) Compared values of the Gaussian distribution for the interaction factor between cells suspended in plasma (black) and PBS (red).

fluctuation characteristics. Both the DFA analysis and autoregressive modeling reveals that the cell is subjected to stress by removing from the natural environment of life (plasma) and resuspension in an artificial environment (PBS), although it largely meets the qualities of the natural environment. The width of the Gaussian distributions show a greater homogeneity of cell population in PBS as a medium for suspension, while the fluctuation in the natural environment is similar for the most cells. We can assume that the homogeneity of cell population in PBS is also due to accelerated aging of cells in an artificial environment.

10.2 Effect of chemicals on the membrane fluctuations

DFA analysis indicates the apparent existence of a *1/f* type power law for the cells suspended in plasma and the cells under the effects of drugs. As we said above, the short range correlation is evident in DFA analysis only for cells suspended in PBS. Averaged power spectra reveal a nonlinear form suitable for modeling with AR1 for all studied cases. The behavior of the spectral correlation exponent, (α), denotes a net separation of the fluctuations behavior for cells suspended in plasma over the washed and suspended in artificial environment cells (see Figure 12 and Figure 11). When cells are suspended in PBS we see a mixing of cell populations (reducing bandwidth Gaussian distribution). It seems that the stress due to the suspension of cells and wash them in an artificial environment is more powerful than the introduction of adrenaline or xiline in their environment. In terms of tress applied to the cell, there are fundamental differences between adrenaline and xiline. Moreover, in PBS all

cells age more quickly, the two parameters (α and φ) having the same behavior. When cells are suspended in plasma, interaction factor decreases from plasma to plasma with xilina, while increasing the degree of heterogeneity of cell populations.

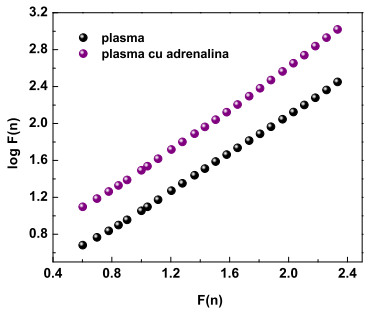

Figure 11: Representation of the averaged DFA for 50 cell suspended in plasma (black) and plasma with adrenaline (lilac). Width fluctuations is enhanced by the existence of adrenaline in suspension medium.

By adding chemicals, such as a hormone (epinephrine) and an anesthetic (lidocaine), we have shown that red blood cell membrane is subjected to additional stress. Fluctuation parameters for plasma (lidocaine $\alpha = 0.97 \pm 0.02$, $\varphi = 0.53 \pm 0.03$, epinephrine $\alpha = 1.09 \pm 0.02$, $\varphi = 0.66 \pm 0.03$) and PBS (lidocaine $\alpha = 1.02 \pm 0.01$, $\varphi = 0.63 \pm 0.02$, epinephrine $\alpha = 0.91 \pm 0.02$, $\varphi = 0.49 \pm 0.02$) suggest that membrane stress is stronger in the case of epinephrine than lidocaine and is similar to that induced by an artificial medium.

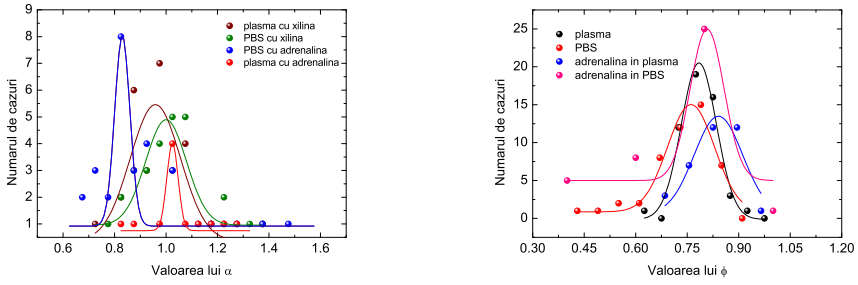

Figure 12: Gaussian fitting of the distribution of spectral correlation exponents (α) for each suspension medium, respectivelly the Gaussian fitting of the interaction factors distribution (φ) for each suspension medium.

The analysis of the interaction factors distribution for different environments shows that the membrane fluctuation are different for each suspension media (see Figure 12). Cells

suspended in plasma have an homogeneous behavior (distribution width is much smaller than in other cases). Cells suspended in PBS have an heterogeneous behavior. Adrenaline and xiline added in suspensions have a much less obvious effect than PBS. In other words we can say that the stress applied by removing the cell from in its natural habitat is more powerful than the administration of drugs.

10.3 Effect of aging *in vitro*

Fluctuation behavior of the membrane where cell aging *in vitro* was investigated by both the DFA and spectral analysis modeled with AR1.

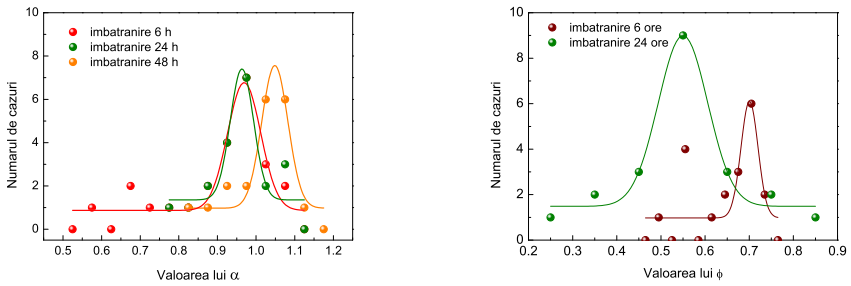

Figure 13: (a) Gaussian distribution of the correlation exponent for aging cell *in vitro* after 6 h, 24 h and 48 h respectivelly. (b) Gaussian of the interaction factor for aging cell *in vitro* after 6 h or 24 h. The behavior of 48 hours aging cells may not be described by a simple AR1 model. It is an $AR_{high-order}$.

Detrended fluctuation analysis shows no significant differences between cells investigated within 6 hours and cells investigated after 24 hours (see Figure 13), $\alpha_{6h} = 0.97 \pm 0.01$ and $\alpha_{24h} = 0.95 \pm 0.01$. Distribution area is 5.59 ± 0.76 for the cells investigated within 6 hours, 6.05 ± 0.47 for cells investigated within 24 hours and 6.59 ± 1.13 for cells investigated within 48 hours. Gaussian distribution shape indicates an increased homogeneity of the cells investigated within 6 hours, those investigated within 24 hours having an heterogeneous behavior. Cells that were investigated within 24 hours also have a heterogeneous behavior, but the law that describes the membranar fluctuations in this case ceases to be of $1/f$ type. A possible explanation about how the fluctuations occur in the case of cells investigated after 48 hours is given by the exhausting the amount of glucose in the suspension medium.

The analytical results are confirmed by autoregressive model (see Figure 13). It should be noted that analysis of 48 hours aging cells could not be done by AR1 modeling, the

fluctuation spectra of these cells being much more complicated. It is a complex model that returns a series of parameters φ which describe together the characteristics of fluctuation. Considering the complexity of the model and the great number of parameters, we preferred to investigate the data series only for cases of aging from 6 hours to 24 hours.

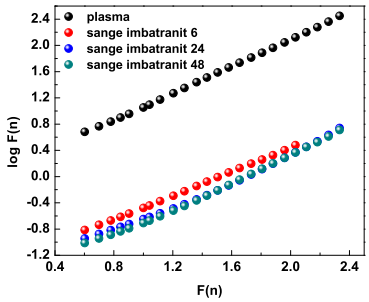

Figure 14: DFA average representation of *in vitro* aging cells. We worked with groups of 50 cells. The fluctuation amplitudes are normal for fresh blood (black) and decrease for 6 hours (red), 24 hours (blue) and respectivelly 48 hours (green) aging blood.

For 6 hours aging cells, the Gaussian distribution median value is 0.70 ± 0.00 for the interaction factor (φ) while for 24 hours it drops to 0.55 ± 0.01. Gaussian area indicates an increased homogeneity at 6 hours, with a value of 5.12 ± 1.56. At 24 hours increased the cell population heterogeneity, with an area of 7.50 ± 0.63.

The representation of the average DFA in case of *in vitro* aging cells shows a net demarcation between fluctuation amplitudes. Cells fluctuates normally when there are analyzed immediately after harvest. After 6 hours, already required glucose whics is almost completely exhausted. There are virtually no differences in terms of amplitude of fluctuation between aging cells 6, 24 or 48 hours.

11 General conclusions

Mathematical methods used to investigate membrane fluctuations are complementary. They return information about the interaction which exists between terms in series and about the mathematical law that govern the flickering phenomenon.

The analysis of the flickering phenomenon of red blood cells indicate the existence of two short range correlation segments. First we remark a very strong correlation between the closer terms. The correlation remains valid for distant terms, although ceases to be of

1/f type.

Cell membrane mobility properties are isotropic, the cell being deformed relatively the same along the large diameter and small diameter. This fact confirmed by correspondence between the values of correlation exponent for area and diameters.

The erythrocytes are rapidly aging in the absence of natural life environment, as evidenced by the rapid drop in spectral correlation exponent when dividing a data series into several equal segments.

Suspension environment affects the way the fluctuation is produced for red blood cells membrane. Cells retain the proper characteristics of fluctuation as long as there are in their natural environment, the blood plasma. Their immersion in an artificial environment, such as PBS (phosphate buffered saline) substantially alter the characteristics of fluctuation.

By adding chemicals, a hormone (epinephrine) and an anesthetic (lidocaine), we have shown that red blood cell membrane is subjected to additional stress. Fluctuation parameters for plasma membrane suggests that the stress is stronger in the case of epinephrine than lidocaine and it is similar to that induced by an artificial suspension medium.

Cellular aging has been emphasized both by detrended fluctuations analysis and autoregressive modeling of power spectra. The methods are so sensitive that one can see differences even for a few minutes.

The experimental results confirmed the theoretical autoregressive modeling. Although apparently erythrocytes membrane fluctuations are of 1/f type, the complementary analysis FFT and autoregressive modeling have shown that the type of correlation which exists in these series is short range. The mathematical law type that defines them best is the autoregressive model of order one.

The mathematical models used to investigate red blood cell membrane fluctuations have been validated by investigating other natural phenomena. For instance, we have shown that the first order autoregressive model (AR1) describes the light radiation emitted from a quasar, and the correlation that exists in the series of lengths of coding sequences of bacterial genomes.

Detrended fluctuation analysis used in conjunction with spectral analysis and autoregressive modeling are a powerful tool that could be used to investigate a wide range of natural phenomena. DFA indicate the type of correlation which exists in series, and, in case of short range correlations, as is the case for most natural phenomena, autoregressive model describes the law that governs them.

References

[1] Jacco Van Uden, Kurt A Richardson, Paul Cilliers, *Postmodernism Revisited? Complexity Science and the Study of Organizations*, Journal of Critical Postmodern Organization Science, Vol 1 (3) 2001.

[2] Cooley, James W., and John W. Tukey, *An algorithm for the machine calculation of complex Fourier series*, Math. Comput. 19: 297-301, 1965.

[3] Thomas H. Cormen, Charles E. Leiserson, Ronald L. Rivest, and Clifford Stein, *Introduction to Algorithms*, 2nd. ed. MIT Press and McGraw-Hill. Especially chapter 30, Polynomials and the FFT, 2001.

[4] Georg Bruun,*z-Transform DFT filters and FFTs*, IEEE Trans. on Acoustics, Speech and Signal Processing (ASSP) 26 (1), 56-63, 1978.

[5] C. M. Rader, *Discrete Fourier transforms when the number of data samples is prime*, Proc. IEEE 56, 1107-1108, 1968.

[6] Leo I. Bluestein, *A linear filtering approach to the computation of the discrete Fourier transform*, Northeast Electronics Research and Engineering Meeting Record 10, 218-219 (1968).

[7] Peng, C.K. et al. *Mosaic organization of DNA nucleotides*, Phys Rev E, 49 (2) 1685-1689, 1994.

[8] Kantelhardt J.W. et al. *Detecting long-range correlations with detrended fluctuation analysis*, Phys A, 295 (3-4) 441-454, 2001.

[9] Zhi Chen, Plamen Ch. Ivanov, Kun Hu, and H. Eugene Stanley, *Effect of nonstationarities on detrended fluctuation analysis*, Phys. Rev. E ,(65) 4, 041107, 2002.

[10] http://en.wikipedia.org/wiki/Detrended-fluctuation-analysis

[11] Vasile V. Morariu, Luiza Buimaga-Iarinca, Calin Vamos, Stefan M. Soltuz, *Detrended Fluctuation Analysis of autoregressive processes*, Fluctuations and Noise Letters 7(3), L249-L255, 2007.

[12] Bunde A. and Havlin S., Eds., *Fractals and Disordered Systems*, Springer, Berlin, Heidelberg, New York, 1996.

[13] Heneghan et al. *Establishing the relation between detrended fluctuation analysis and power spectral density analysis for stochastic processes*, Phys Rev E, 62 (5) 6103-6110, 2000.

[14] A.N. Shiryaev, *Probability*, 2nd ed., Springer, pages 405 and 409, 1996.

[15] Priestley, M.B. *Spectral Analysis and Time Series*, Academic Press, 1981.

[16] Priestley, M.B. *Non-linear and Non-stationary Time Series Analyis*, Academic Press and Physical Review E, vol. 64, 011114, 2001(1988).

[17] Kun Hu, Plamen Ch. Ivanov, Zhi Chen, Pedro Carpena, and H. Eugene Stanley, *Effect of Trends on Detrended Fluctuation Analysis*, Physical Review E, vol. 64, 011114, 2001.

[18] Mills, Terence C. *Time Series Techniques for Economists*. Cambridge University Press, 1990.

[19] Percival, Donald B. and Andrew T. Walden, *Spectral Analysis for Physical Applications*, Cambridge University Press, 1993.

[20] Pandit, Sudhakar M. and Wu, Shien-Ming, *Time Series and System Analysis with Applications*, John Wiley and Sons, Inc., 1983.

[21] G. Udny Yule *On a Method of Investigating Periodicities in Disturbed Series*, with Special Reference to Wolfer's Sunspot Numbers, Philosophical Transactions of the Royal Society of London, Ser. A, Vol. 226, 267-298, 1927.

[22] G. E. P. Box and G. M. Jenkins, *Time Series Analysis: Forcasting and Control*, 2nd ed. Holden-Day, San Francisco, 1976.

[23] P.J. Brockwell and R. Davis, *Time Series: Theory and Methods*, Springer-Verlag, New York, 1991.

[24] P.J. Brockwell and R. Davis, *Introduction to Time Series and Forecasting*, Springer-Verlag, New York, 1996.

[25] J.D. Hamilton, *Time Series Analysis*, Princeton University Press, 1994.

[26] P. Stoica and R. L. Moses, *Introduction to Spectral Analysis*, Prentice-Hall, New Jersey, 1997.

[27] Calin Vamos, Stefan M. Soltuz, Maria Craciun, *Order 1 autoregressive process of finite length*, arXiv:0709.2963v1 [physics.data-an]

[28] MATLAB R2008a, http://www.mathworks.com/

[29] W. Li, *A Bibliography on 1/f Noise (1996 - present)* http://www.nslij-genetics.org/wli/ 1fnoise /

[30] A. Coza and V.V. Morariu, *Generating 1/f noise with a low dimensional attractor characteristic: its significance for atomic vibrations in proteins and cognitive data*, Physica A 320, 449-460, 2001.

[31] Th. L. Thornton and D. L. Gilden, *Provenance of correlations in psychological data*, Psychonomic Bul. Rev. 12, 409-441, 2005.

[32] Elsworth, Y.P., James, J.F. *The flicker spectrum of AE Aquarii*, Mon. Not. R. Astr. Soc., 198, 889-896, 1982.

[33] Lochner, J.C., Swank, J.H., Szymkowiak, A.E. *Shot model parameters for Cygnus X-1 through phase portrait fitting*, Astrophys. J., 376, 295-311, 1991.

[34] Smith, M.A., Robinson, R.D. *Interplay of periodic, cyclic and stochastic variability in selected areas of the H-R diagram*, ASP Conf. Ser., 292, 263-274, 2003.

[35] Gaskell, C.M., Klimek, E.S. *Variability of active galactic nuclei from the optical X-ray regions*, Astron. Astrophys. Trans., 22, 661-679 2003.

[36] Uttley, P., McHardy, I.M. *The Flux-dependent amplitude of broadband noise variability in X-ray binaries and active galaxies*, Mon. Not. R. Astr. Soc., 323, L26L30, 2001.

[37] Papadakis, I.E., Lawrence, A. *A detailed X-ray variability study of the Seyfert galaxy NGC 4051*, Mon. Not. R. Astr. Soc. 272, 161-183, 1995.

[38] McHardy, I.M., Papadakis, I.E., Uttley, P., Page, M.J., Mason, K.O. *Combined long and short time-scale X-ray variability of NGC 4051 with RXTE and XMM-Newton*, Mon. Not. R. Astr. Soc., 348, 783-801, 2004.

[39] Konig, M., Timmer, J. *Analyzing X-ray variability by linear state space models*, Suppl. Ser., 124, 589-596, 1997.

[40] Vamos, C. *Automatic algorithm for monotone trend removal*, Phys. Rev. E, 75, 036705, 2007.

[41] D. J. Li, S. Zhang, *The C -value enigma and timing of the Cambrian exposion*, arXiv Preprint Archive [on line], http://arxiv org/abs/0806.0108, 2008.

[42] D. J. Li, S. Zhang, *Prediction of genomic properties and classification of life by protein length distributions*, arXiv Preprint Archive [on line], http://arxiv org/abs/ 0806.0205, 2008.

[43] D. J. Li, S. Zhang, *Classification of life by the mechanism of genome size evolution*, arXiv Preprint Archive [on line], http://arXiv org/abs/0811.3164, 2008.

[44] Y. Zhuang, F. Ma, J. Li-Ling, X. Xu, Y. Li, *Comparative analysis of amino acid usage and protein length distribution between alternatively and non-alternatively spliced genes across six eukarotic genomes*, Mol.Biol. Evol. 20 (12) 1978-1985, 2003.

[45] A. L. Berman, E. Kolker, E. N. Trifonov, *Underlying order in protein sequence organization*, Proc. Natl. Acad. Sci. USA 91 4044-4047, 1994.

[46] B. Rost, *Did evolution leap to create the protein universe?*, Curr.Opin.Stru, Biol 12 409-416, 2002.

[47] O. Zainea, V. V. Morariu, *The length of coding sequences in a bacterial genome: evidence for short-range correlation*, Fluct. Noise Lett. 7 501-508, 2007.

[48] B. B. Mandelbrot, *Multifractals and 1/f noise*, Springer, New York 1998.

[49] V. V. Morariu, C. Vamos, A. Pop, S. M. Soltuz, L. Buimaga-Iarinca, O. Zainea, *Autoregressive description of biological phenomena* arXiv Preprint Archive, http://arxiv org/abs/0808.1021, 2008.

[50] O. Zainea, V. V. Morariu, *A correlation investigation of bacterial DNA coding sequences*, Romanian J. Biophys. 18 19-28, 2008.

[51] E. P. C. Rocha, *The replication-related organization of bacterial genomes*, Microbiology 150, 1609-1627, 2004.

[52] F. Kunst, N. Ogasawara, I. Moszer and 148 other authors. *The complete genome sequence of the Gram-positive bacterium Bacillus subtilis*, Nature 390, 249-256, 1997.

[53] F. R. Blattner, G. Plunkett, I. C. A.Bloch and 14 other authors, *The complete genome sequence of Escherichia coli K-12*, Science 2 77, 1453-1461, 1997.

[54] E. P. C Rocha, A. Danchin *Competition for scarce resources might bias bacterial genome composition*, Trends Genet 18, 291-294, 2002.

[55] Kuchel, Philip W., Ralston, Gregory B., Berstein, Audrey M., Easterbrook-Smith, Simon B, *Schaum's Outline of Theory and Problems of Biochemistry* 2nd ed, McGraw Hill, New York, 1997.

[56] R.H.Garrett C.M.Grisham, *Biochemistry*, 2nd ed, Harcourt, Florida, 1999.

[57] Peter Mulquiney, Philip W. Kuchel, *Modelling Metabolism with Mathematica: Analysis of Human Erythrocyte*, CRC Press, Boca Raton, 2003.

[58] http://images.google.ro /imgres?imgurl=http :// kentsimmons.uwinnipeg.ca/ cm1504/ Image127.gif

[59] Singer S.J., Nicolson G.L., *The fluid mosaic model of the structure of cell membranes*, Science 175 (23): 72031, 1972.

[60] Alberts B., Johnson A., Lewis J., *et al.*, *Molecular Biology of the Cell* (4th ed.), New York: Garland Science, 2002.

[61] David Szekely, *Chemical and physical dynamics of cells: the calcium oscillator in hek-293 cells and erythrocyte rapid membrane transport and flickering*, Phd Thesis, University of Sydney, Australia, 2009.

[62] http://www.itg.uiuc.edu/exhibits/iotw/2008-11-18/

[63] Laura Dean *Blood Groups and Red Cell Antigens*, http://onlinebooks. library.upenn.edu/ webbin/book/ lookupid?key= olbp36833

[64] Pierig F, Serafini S, Rossi L, Magnani M , *Cell-based drug delivery*, Advanced Drug Delivery Reviews 60 (2): 28695, 2008.

[65] Kabanova S, Kleinbongard P, Volkmer J, Andre B, Kelm M, Jax TW, *Gene expression analysis of human red blood cells*, International Journal of Medical Sciences 6 (4): 1569, 2009.

[66] Hillman, Robert S., Ault, Kenneth A., Rinder, Henry M., *Hematology in Clinical Practice: A Guide to Diagnosis and Management* (4 ed.), McGraw-Hill Professional. p. 1, 2005.

[67] University of Virginia Pathology, *Iron Metabolism* Accessed 22 September 2009.

[68] Kenneth R. Bridges, *Iron Transport and Cellular Uptake*, Information Center for Sickle Cell and Thalassemic Disorders. Accessed 22 sept 2009.

[69] Fller M, Huber SM, Lang F, *Erythrocyte programmed cell death*, IUBMB Life 60 (10): 6618, 2008.

[70] Elgsaeter A., Mikkelsen A., *Shapes and shape change in vitro in normal red blood cells*, Biochim.Biophys.Acta, 1071, 273-290, 1991.

[71] Zeman K., Engelhard H., Sackmann E. *Bending undulations and elasticity of the membrane: effects of cell shape and membrane organization*, Eur.Biophys. J., 1990.

[72] Tuvia S. Levin, S. Korenstein R. *Correlation between local membrane displacements and filterability of human red blood cells* FEBS Lett. 304, 32-36, 1992.

[73] Tuvia S. Levin S. Korenstein R., *Oxygenation-deoxygenation cycle of erythrocytes modulates submicron cell membrane fluctuations*, Biophys. J. 63, 599-602, 1992.

[74] Strey H. Peterson, M. Sackmann E. *Measurement of erythrocyte membrane elasticity by flicker eigenmode decomposition* Biophys. J. 69, 478-488, 1995.

[75] Tuvia S. Almagor A. Bittler A. Levin S. Korenstein R. Yedgar S, *Cell membrane fluctuations are regulated by medium macroviscosity evidence for a metabolite driving force* Proc.Nat.Acad.Sci USA 94, 5045-5049, 1997.

[76] Tuvia S. Levin S. Bitles A. Korenstein R., *Mechanical fluctuations of the membrane -skeleton are dependent on F-actin ATPase in human erythrocytes* J.Cell Biol. 141 1551-1561, 1998.

[77] Alster Y. Loewenstein A. Levin S. Lazar M. Korenstein R., *Low-frequency submicron fluctuations of red blood cells in diabetic retinopathy*, Arch.Ophtalmol. 116 1321-1325, 1998.

[78] Gaczinska M., Barotsz G., *Oscillations in erythrocyte membrane preparations*, Cytobios, 52 93-98, 1987.

[79] Peleg L. Dotan A. Luzato P. Ashkenazi I.E., *Long ultradian rhythms in red blood cells and ghost suspensions; possible involevement of cell membrane* In Vitro Cell Dev. Biol. 26, 978-982, 1990.

[80] Popescu G., Deflores L. P., Vaughan J. C., P*Fourier phase microscopy for investigation of biological structure and dynamics*, Optic Letters, Vol 29., No 21, 2004.

[81] Popescu G., Ikeda T., Best C. A., Badizadegan K., Dasari R.R., Feld M., *Erythrocyte structure and dynamics quantified by Hilbert Phase Microscopy*, JBO Letters, Vol 10(6), 2005.

[82] Popescu G., Ikeda T., Dasari R. R., Feld M., *Diffraction phase microscopy for quantifying cell structure and dynamics*, Optic Letters, Vol 31 No 6, 2006.

[83] Lue N., Choi W., Popescu G., Ikeda T., Dasari R., Badizadegan K., Feld M., *Quantitative phase microscopy of live cells using Fast Fourier Phase Microscopy*, Applied Optics Vol 46 No 10, 2007.

[84] Popescu G., Badizadegan R., Dasari R., Feld M., *Observation of dynamic subdomains in red blood cells*, Journal of Biomedical Optics, Vol 11(4), 2006.

[85] Popescu G., Park Y., Dasari R., Badizadegan K., Feld M., *Coherence properties of red blood cell membrane motions*, Phys Rev. E, Vol 76(3), 2007.

[86] http://en.wikipedia.org/wiki/File:Erythrocyte Membrane lipids.jpg

[87] http://www.optikamicroscopes.com/prod/XDS2.asp

[88] http://www.optikamicroscopes.com/prod/TECH/OPTIKAM-TECH-PRO.asp

[89] Rasband, W.S., ImageJ, U. S. National Institutes of Health, Bethesda, Maryland, USA, http://rsb.info.nih.gov/ij/, 1997-2006.

[90] Abramoff, M.D., Magelhaes, P.J., Ram, S.J. *Image Processing with ImageJ*, Biophotonics International, volume 11, issue 7, pp. 36-42, 2004.

[91] Syverud, K., Chinga, G., Johnssen, P.O., Leirset, I. and Wiik, K. *Analysis of lint particles from full-scale printing trials*. Appita J. 60(4): 286-290, 2007.

[92] Russ, J.C., *The image processing handbook*, CRC Press, USA (1999).

[93] Foley, James D.; Andries van Dam, John F. Hughes, Steven K. Feiner, *Spatial-partitioning representations; Surface detail. Computer Graphics Principles and Practice*, The Systems Programming Series, Addison-Wesley, 1990.

[94] L Buimaga-Iarinca, V.V. Morariu, *Phosphate Buffered Saline-induced changes in red blood cells membrane fluctuations*, Studia UBB, Physica LIII(2), 2008.

[95] L Buimaga-Iarinca, *Autoregressive analysis of the erythrocyte flickering*, Rom. J. Biophys 18(1), 67-72, 2008.

[96] L Buimaga-Iarinca, V Morariu, *Short range correlation of the erythrocyte membrane fluctuations*, Journal of Physics: Conference Series 182, 012005 doi:10.1088/1742-6596/182/1/012005, 2009.

[97] Erika Check Hayden, *Age research: A new angle on old*, Nature 450, 603-605, doi:10.1038/450603, 2007.

[98] Jacob, F., Perrin, D., Sanchez, C. and Monod, J., *Operon: a group of genes with the expression coordinated by an operator*, C. R. Hebd. Seances Acad. Sci., Vol. 250, pp. 17271729, 1960.

Index